Dietary strategies of Pleistocene *Pongo* sp. and *Homo erectus* on Java (Indonesia)

Jülide Kubat (julide.kubat@parisdescartes.fr)
Université de Paris https://orcid.org/0000-0002-8772-5172

Alessia Nava
Skeletal Biology Research Centre, School of Anthropology and Conservation, University of Kent; Diet and ANcient TEchnology Laboratory, Department of Maxillo-Facial Sciences, Sapienza University
https://orcid.org/0000-0002-6319-0425

Luca Bondioli
Museum of Civilization

Christopher Dean
University College London

Clément Zanolli
Université de Bordeaux https://orcid.org/0000-0002-5617-1613

Nicolas Bourgon
Max Planck Institute for Evolutionary Anthropology

Anne-Marie Bacon
Paris Descartes University

Fabrice Demeter
Lundbeck Foundation, GeoGenetics Centre, Globe Institute, University of Copenhagen

Beatrice Peripoli
University of Padova

Patrick Mahoney
University of Kent

Richard Albert
Institute of Geosciences Goethe University Frankfurt https://orcid.org/0000-0002-0185-8581

Ottmar Kullmer
Senckenberg Research Institute Frankfurt a.M. https://orcid.org/0000-0002-5929-8070

Friedemann Schrenk
Johann Wolfgang Goethe University

Wolfgang Müller
Institute of Geosciences Goethe University Frankfurt

Article

Keywords: Pleistocene, Homo erectus, Pleistocene Pongo sp., diet

Posted Date: October 1st, 2021

DOI: https://doi.org/10.21203/rs.3.rs-940427/v1

Version of Record: A version of this preprint was published at Nature Ecology & Evolution on January 16th, 2023. See the published version at https://doi.org/10.1038/s41559-022-01947-0.

Abstract

During the early Pleistocene, Java was inhabited by a high variety of hominid and hominin taxa with hitherto unclear seasonal dietary demands. We undertook the first geochemical analyses of Pongo sp., Homo erectus and mammalian Pleistocene teeth from Sangiran. We reconstructed past dietary strategies at daily resolution and inferred sub-seasonal ecological patterns. Histologically-controlled spatially-resolved elemental analyses by LA-ICPMS, confirmed the preservation of authentic biogenic signals despite very weak diagenetic overprint. The Sr/Ca record of mammals is in line with expected trophic positions, contextualizing fossil hominid diet. Herbivorous Pongo sp. displays marked seasonal cycles with ~3-month-long strongly elevated Sr/Ca peaks, reflecting highly nutritional plant food during monsoon seasons. Lower Sr/Ca signals suggest different food availability during the dry season. In contrast, omnivorous Homo erectus shows low and less accentuated intra-annual Sr/Ca variability. We infer that Homo erectus maintained its nutritional demands independent of seasonal fluctuations by exploiting the regional diversity of high-quality food resources.

Background

The Pleistocene hominid fossil record from the Sangiran Dome in Central Java, Indonesia, is one of the largest palaeoanthropological collections in Southeast Asia, evidencing an Early Pleistocene expansion of *Homo erectus* onto the Sunda Shelf[1–4]. The high morphodimensional variability of hominid specimens attributed to a variety of taxa such as *Homo erectus*, *Meganthropus palaeojavanicus, Pithecanthropus dubius* or *Pongo* sp. fueled taxonomic debates[1,5–9]. Recently, a high level of Javanese hominid palaeodiversity was revealed, which confirmed the taxonomic validity of the genus *Meganthropus*, a taxon that coexisted with *H. erectus* and *Pongo*[10]. Although dental macrowear and enamel thickness broadly reflect different dietary adaptations among these hominids, little is known about their detailed ecological niches and their inter- and intraspecies competition[10].

Previous geochemical analyses of tooth enamel provided insights into palaeoenvironment, palaeodiet and life history of extinct hominins such as *Australopithecus*[11,12], *Paranthropus*[11] and Neanderthals[13,14]. Tooth enamel – contrary to bone and dentine – is less prone to post-mortem diagenetic alteration due to its highly mineralized nature[15,16]. Moreover, it mineralizes sequentially in utero and during early infancy and, once formed, remains compositionally and structurally stable during life. Consequently, enamel captures and preserves environmental and dietary changes that occur during the enamel mineralization phases in an individual's life[17–20]. Laser-Ablation Inductively-Coupled-Plasma Mass Spectrometry (LA-ICPMS) analysis of the chemical composition across the incremental structures of sequentially secreted enamel provides a temporally and spatially highly-resolved record of an individual's childhood. Such data allow the interpretation of diet, health, growth rates, weaning, and mobility as well as changes of the environmental setting on a seasonal to even daily scale[13,14,21–23]. Besides stable carbon isotope ratios (e.g. $\delta^{13}C$ values), trace element ratios (Sr/Ca, Ba/Ca) in dental enamel can record dietary signals due to the biopurification of Ca in trophic chains[24–26]. The higher the

trophic level, the less [Sr] and [Ba] relative to [Ca] are incorporated into enamel, resulting in higher trace element ratios in herbivore enamel than that of omnivores or carnivores[11,24,27], though additional factors such as soil ingestion play a role[28].

Previous stable isotope analysis of *H. erectus* samples from Sangiran were not successful in obtaining palaeoecological signals due to diagenetic alteration of bone tissue[29]. To assess dietary and life history signals in penecontemporaneous *H. erectus* and ancestral orang-utan from Southeast Asia, we explored strontium/calcium (Sr/Ca) and barium/calcium (Ba/Ca) ratios and other elemental signals at high spatial/time-resolution in dental enamel of premolars and molars from Sangiran. For comparison and as trophic level reference we utilized isolated premolars and molars from several large mammal families (Cervidae, Rhinocerotidae, Hippopotamidae, Suidae, Felidae) from the Sangiran fossil assemblage (Table 1). We focused our study on Sr/Ca (and to a lesser extent Ba/Ca) ratios as (relative) trophic level proxies, including an assessment of how well biogenic geochemical information is preserved in Mid-Pleistocene bioapatite from (sub)tropical contexts by utilizing elements Mn, Al, Y, Ce, U as tracers for post-mortem alteration[14,27,28,30,31].

Results

Table 2 reports crown formation time, Retzius periodicity (RP) and laser track length of all investigated samples. The RP of *Pongo* sp. F8864 was obtained through direct counts of cross striations between two adjacent Retzius lines. *Homo erectus* RP, given the section thicknesses necessary for chemical analyses and the presence of some accentuated markings, was calculated as the distance between adjacent Retzius lines divided by local daily secretion rate (DSR).

Elemental signals were retrieved within enamel closest to the enamel-dentine-junction (EDJ; approx. <100µm) because it is where initial environmental signals are best captured topographically and elemental overprint during enamel maturation has the least effect [14,22,32–34]. For assessing post-mortem diagenetic overprint scatterplots of Sr/Ca or Ba/Ca vs. [Mn] or [U] concentrations at EDJ profiles of representative samples of each trophic level were generated (Fig. 1 and Supplementary Fig. 3). All cases show clearly positive correlations between proxy and diagenesis-indicating elements. Even though multi-stage diagenetic histories may be indicated by different trajectories (Fig. 1), uptake of [Sr] and [Ba] with increasing geochemical alteration is evident, which implies that the best approximations of initial biogenic [Sr] or [Ba] (or expressed as Sr/Ca, Ba/Ca ratios) can be found at lowest [Mn] or [U]. These plots also reveal that [Sr] increases by 40-80%, while Ba is characterized by a threefold to tenfold increase, confirming the higher susceptibility of Ba to post-mortem overprint. Repeat profiles at both EDJs or corresponding EDJ and prism orientation indicate greater consistency between corresponding Sr/Ca profiles, relative to those of Ba/Ca (Supplementary Fig. 4). Using [Mn] and [U] thresholds of 400 and 1 ppm, respectively, to screen Sr/Ca and Ba/Ca trophic level signals, reveal expected patterns for trophic groups for Sr/Ca, but more ambiguous ones for Ba/Ca (Fig. 2; Supplementary Fig. 4). As a result, we

focus more on Sr/Ca results but also note that Ba/Ca can indicate apparently reliable results in case of well-preserved samples (see below).

The Sr/Ca ratio boxplots of faunal and hominid specimens show carnivorous Felidae with the lowest Sr/Ca ratio in the faunal assemblage (~$8.4*10^{-4}$), following the expected trophic level trend towards lower Sr/Ca ratios relative to omnivores ($1.1*10^{-3}$; represented by Suidae) and different herbivore groups ($1.6*10^{-3}$ – $4.0*10^{-3}$). Rhinocerontidae exhibit a Sr/Ca level ~2 times higher than all other herbivores and a large Sr/Ca variability. The three *Homo erectus* dental specimens yield Sr/Ca ratios between those of the Felidae and Suidae. The *Pongo* sp. specimen F8864 shows the by far widest Sr/Ca distribution among all taxa and has a large number of distributional outliers toward higher Sr/Ca values. The median value fits well within the Hippopotamidae and Cervidae central distributions. The peculiar distribution of Sr/Ca values in *Pongo* sp. F8864 is the result of distinct Sr/Ca peaks throughout the life of this individual (see below).

For the hominid samples, the elemental ratio profiles were aligned with the individual odontochronologies (see Supplementary Figures 5 and 6) on both lingual and buccal aspects (except for S7-37 P^4 where only the buccal aspect was available for analysis) to derive Sr/Ca (and Ba/Ca) variability vs time (secretion-days). Fig. 3a shows the Sr/Ca and Ba/Ca EDJ profiles together with diagenesis-indicating [U] and [Mn] against time for the 1073 days (2 years and 11 months) of the buccal aspect of the *Pongo* sp. F8864 molar. EDJ and corresponding prism (P) Sr/Ca profiles for the buccal enamel are compared in Fig. 3b, which show good agreement but invariably lower Sr/Ca values towards outer enamel along the prisms. Both Sr/Ca EDJ profiles (buccal, lingual) are contrasted against one another in Fig. 3c. The time span covered by the two LA profiles is 1073 days (2 years and 11 months) on the buccal aspect and 1339 days (3 years and 8 months) on the lingual one (Fig. 3), corresponding to the entire crown formation time. [Mn] and [U] on both sides of the crown are at detection limit for the most part, with [U] rising to <2 ppm for the final ~100 days of thin cervical enamel. Neither Sr/Ca nor Ba/Ca ratio is strongly affected by these minor U increases confirming the biogenic nature of the signal; yet we note that some smaller Ba/Ca-peaks co-occur with minor U-peaks (e.g. ~930 days; Fig. 3a). Enamel incremental growth parameters such as crown formation time (CFT) for F8864 yielded 1125.2 days.

The consistency of the chronologies is attested by the high correspondence of the Sr/Ca signals between the two EDJ and prisms profiles. *Pongo* sp. F8864 exhibits stark intra-tooth variability with three distinct peaks characterized by up to sixfold Sr/Ca and ~eightfold Ba/Ca increases. This sixfold Sr/Ca change for the first peak ($1.8*10^{-3}$ to $10.7*10^{-3}$) decreases for the second and third peaks to threefold and twofold values, respectively. The influence of the Sr/Ca attenuation along prisms towards outer enamel[22] is discernible but partly compensated for in e.g. prism 3 by the strong biogenic signal (Fig. 3b).

On the buccal side, three hypoplastic defects and four accentuated lines (AL) are present (´Fig. 3c), yet all growth disturbances[35] are not coincident with the Sr/Ca (or Ba/Ca) variability. The interval between the midpoints of two consecutive peaks on the buccal aspect approximates one year, namely 364 and 324 days between peaks 1-2 and peaks 2-3, respectively. The duration of these peaks is 95, 118 and 90

relative days for the first, second and third peak, respectively, approximating an overall duration of approximately three months each.

The Sr/Ca-profiles of the three *H. erectus* samples display low [U] and [Mn] and thus acceptable preservation, apart from localized peaks indicating spatially-restricted diagenetic alteration (Fig. 4). Comparative elemental profiles for the lingual and buccal aspects of two *H. erectus* specimens presented in Supplementary Figures 5 and 6, illustrate that enamel of the same tooth may be variably preserved yet we utilize the better preserved domains. Limited inter-sample Sr/Ca-variation ranges between 0.7-1.4*10^{-3}, while intra-profile Sr/Ca-variability is 20-30%. These *H. erectus* Sr/Ca-values are thus always below those in *Pongo* sp. F8864, which is even more pronounced for the intra-sample variability (20-30 vs. 200-600%). The temporal spacing between broad Sr/Ca troughs and/or peaks in all samples lies between 340-380 days, consistent with approximately annual cyclicity. As it is uncertain which of the apparent minor Sr/Ca fluctuations are indicative of variable food intake or minor kryptic diagenetic overprint, we refrain from attributing unwarranted importance to small-scale variability. CFTs for F8865, S7-13 and S7-37 are 662.8, 668.9 and 1050 days, respectively.

Discussion

Hominid Retzius periodicity and cusp formation times. Retzius periodicities of 7 to 9 days for our sample of *Homo erectus* teeth are typical of these early humans. They are similar to the periodicities reported previously for *Homo erectus/ergaster* molars and premolars (7-8 and 9 days, respectively)[36], but this apparent tighter distribution of values differs from the wider range of periodicities between 6 to 12 days characteristic of larger samples of living humans[37]. An 8-day periodicity for the *Pongo* sp. lower molar F8864 is slightly lower than the 9 to 12-day periodicity reported for fossil *Pongo* from Sumatra and mainland Asia[38] but lies within the range of values (8-11 days) reported for living *Pongo*[39].

Hominid trophic levels at Sangiran. Trophic levels portray the relative position of species in a food web and are important for ecosystem functioning[40]. Fossil teeth of penecontemporaneous Carnivora (Felidae), Perissodactyla (Rhinocerotidae), and Artiodactyla (Suidae, Cervidae, Hippopotamidae) with known trophic levels were used to establish an underlying trophic level framework for Sangiran. It confirmed that Sr/Ca is a reliable trophic level indicator that shows negligible post-mortem diagenetic alteration. Additionally, this approach allowed to successfully assess the diet of the specimens even in the absence of stratigraphic context. The ordering of fossil faunal taxa from Sangiran according to their enamel Sr/Ca ratios ($Sr/Ca_{carnivores}$<$Sr/Ca_{omnivores}$<$Sr/Ca_{mixed\text{-}feeder}$<$Sr/Ca_{grazers}$) reflects trophic level differences that are in good agreement with their expected dietary habits (Fig. 2)[11,41], suggesting reliable trophic level determination based on enamel Sr/Ca.

The *Pongo* sp. lower molar F8864 exhibits a predominantly plant-based diet as evidenced by a high intra-tooth variability for Sr/Ca ratios along the EDJ profile (Fig. 3) covering the whole range of the herbivorous

specimens in this study (Fig. 2). The average Sr/Ca ratios between the peaks is closer to the Sr/Ca ratio of mixed-feeding animals such as *Hexaprotodon* sp. and *Axis lydekkeri*[42–45]. The maximum Sr/Ca values for the first and second peaks are even higher than those of the rhinocerotids, which are predominantly grazers[46].

The *H. erectus* lower molar F8865 shows Sr/Ca ratios similar to *H. erectus* individuals S7-13 and S7-37. All *H. erectus* specimens in this study group with omnivorous (Suidae) and carnivorous (Felidae) mammals from Sangiran (Fig. 2), suggesting an omnivorous diet with a certain degree of meat consumption for *H. erectus* on Java. There is broad agreement that early *Homo* gradually increased the meat content in the diet[47], and an increasly carnivorous diet over time for *H. erectus* is probable[48,49].

Comparison of Sr/Ca patterns in *Homo erectus* and *Pongo* sp. The biogenic Sr/Ca peaks in *Pongo* sp. F8864 occur on a nearly annual basis (Fig. 3). The first and the second peaks are approximately 364 days apart, and 324 days for the second and last peaks. The first peak is located in the cuspal area of the EDJ profile and displays the highest amplitude with a signal approximately 6 times higher than the baseline Sr/Ca values. The amplitude of peaks decreases towards the cervical margin of the tooth.

The Sr/Ca variation in *H. erectus* F8865 also shows a cyclical pattern: the duration of the first cycle is approximately 320 relative days and the second one 261 relative days. The first cycle ends with a strong decrease of Sr/Ca after 320 relative days and the second cycle with a less proniunced decrease of Sr/Ca relative to the elevated parts of the Sr/Ca signal. *H. erectus* S7-13 shows a complete cycle of 347 relative days and a partial cycle of 148 days. The development of the crown was completed before the cycle was finished. *H. erectus* S7-37 also shows two cycles with a duration of 375 relative days and 383 relative days. The second cycle is marked by two smaller Sr/Ca decreases within the cycle. Uranium is not following the annual cycle trend in any of the samples (Fig. 4a-c).

In summary, all *H. erectus* individuals demonstrate two low-amplitude Sr/Ca cycles with a duration of approximately one year, whereas *Pongo* sp. F8864 demonstrates two cycles with sharp peaks that last 3-4 months.

Diet of *Pongo* sp. reflects high seasonal food variability. The Sr/Ca and Ba/Ca ratios of *Pongo* sp. F8864 show a cyclical pattern with incidences of higher ratios occuring on an essentially annual basis (Fig. 3). The gradual decrease of the Sr/Ca and Ba/Ca peaks within the ~3 years of life represented by the tooth may be explained via the development of stronger metabolic biopurification processes and increasing gut maturation, which develop with age[50,51]. [Sr] and [Ba] as non-essential elements characterized by larger ionic radii (especially Ba) are metabolically discriminated through the biopurification of essential elements such as [Ca][30]. It was observed that young mammals are less efficient in discriminating [Sr] than adults[50]. Gastro-intestinal discrimination against [Sr] in modern humans for instance is not

completely matured until late infancy or adolescence[51–53]. Enamel mineralization in *Pongo* sp. F8864 approximately took place between the 3rd to 6th year, with the third peak corresponding close to 5.5 years in the life time of the individual (Fig. 3). The low amplitude of the last peak might be a result of these stronger metabolic biopurifaction processes and increased gut maturation since orangutans reach adolescence on average around 7 years of age, with the termination of breast-feeding[54,55].

The repeatedly high Sr/Ca and Ba/Ca signals in our samples likely reflect annual periods with an increased intake of peculiar plant-based food resources, probably linked to a higher food availability during monsoonal periods and mast-fruiting events, with a variation of the peaks linked to variability in intensity[56]. Studies of palaeosols and the occurrence of palaeovertisols in the Sangiran Dome strongly suggest that Java was a monsoon region in the Early Pleistocene, with an annual dry season[3].

Recent studies suggested causal relationships to a cyclical nursing pattern, which results in a cyclical increase of Ba concentrations in teeth (i.e., an increase intake on mothers' milk)[57]. However, the synchronous up to sixfold in Sr/Ca and up to eightfold increase Ba/Ca signals are unlikely to reflect a breastmilk signal because of depletion of breast milk Sr due to epithelial discrimination in mammary glands[14,22,53].

The relatively longer duration of low Sr/Ca signals between peaks most likely reflects periods of different, likely lower food availability during dry seasons, moreover when infants are generally nursed[57]. Recent studies on cementum in *Pongo* revealed that regions of [Sr] enrichment and depletion relate to seasonal fluctuations in diet rather than cyclical breastfeeding[58,59]. Calorific intake in orangutans is 2-3 times greater during masting events[56], which are usually followed by periods of low fruit availability during dry periods, compensated in turn by burning fat reserves stored during mast-feeding[60]. Sr/Ca and Ba/Ca signals might also be enhanced during episodes of mast-feeding because of geophagic behaviour, the deliberate ingestion of soils enriched in trace elements, which absorb toxins and tannins[59]. This behaviour was previously observed in orangutans[61]. Geophagy combined with the high availability of food resources during monsoonal seasons might be the reason for the high signal intensity of Sr/Ca and Ba/Ca.

Accentuated lines, occurring between the first and the second peaks (Fig. 3c) provide further evidence of seasonal effects, as they reflect stress events related to malnutrition or metabolic changes during illness probably occurring more frequently during dry seasons. A further sign of physiological stress is hypoplastic defects on the tooth crown. Although they do not exactly follow the peaks in every single instance (Fig. 3c), they clearly indicate developmental deficiencies, potentially caused by malnutrition and/or illness[14,35].

Our observations are linked to inhabiting tropical rainforests, which are cyclical in terms of food availability, reflecting an ecologically challenging environment for infants[35,62,63]. Orangutans have the slowest life histories of any non-human primates with the latest weaning age of any mammals at around

7 years, but with relatively low levels of nutrient transfer during breast-feeding[54,55,57,64]. Consequently, solid foods are supplemented in the infant's diet between 12 and 18 months of age, to compensate additional nutritional demands[55,57]. Infants can forage solid foods independently from the age of ~1.5 years, whilst the mother is not decreasing her lactation efforts[55]. Dry seasons with low food availability are compensated by extending weaning ages for infants leading to low growth and reproduction rates and solitary lifestyles[60,62,65,66].

***Homo erectus* alleviated effects of seasonal food variability.** All *H. erectus* specimens investigated show two distinct Sr/Ca cycles with a duration of approximately one year (Fig. 4). It is unlikely that these cycles represent breast-feeding signals or weaning stress as the estimated ages for tooth development in the analysed *H. erectus* teeth exceed the expected weaning time[67]. Since ages for P4, M1, M2 and M3 tooth formation in *H. erectus* falls in the range of modern humans[68], we may assume a weaning age for *H. erectus* comparable to modern humans.

In contrast to the results from *Pongo* sp. the yearly Sr/Ca cycles in *H. erectus* do not indicate substantial (sub-)seasonal dietary changes. This is evidenced by the low amplitude of Sr/Ca cycles (20-40%), which is much smaller than the seasonal changes observed in *Pongo* sp. F8864. For *H. erectus*, these might reflect the consumption of specifically selected animal or plant resources, which were available in the regional context of a highly diverse ecosystem. Lowland rain forest was the major vegetation of Central Java during the Early Pleistocene[69,70]. Oscillations of humid and dry phases led to fragmentation and opening of the rain forests and the spreading of grasslands, including the occurrence of several months-long dry seasons[71].

The larger brain size of *H. erectus* may have required the consumption of energy-rich food sources such as meat and marrow[72–76]. *H. erectus* was using tools to access these high quality foods[77] In analogy to "mobility events" known from recent hunter-gatherers[78,79], *H. erectus* might have exploited regionally available resources. In general, a high adaptive versatility is assumed for early members of the genus *Homo*[80]. In addition, dental microwear traits in Sangiran *H. erectus* teeth also confirm an opportunistic omnivorous dietary strategy[81,82].

The duration of the sub-annual Sr/Ca cycles observed in *H. erectus* from Sangiran could result from logistical movements where the maximum of available resources are exploited within the location of the residential camp. As soon as food resources were exhausted, the group moved to new living grounds. This transitional period of residential movements[78,79] could be responsible for the major fluctuations in Sr/Ca ratios. The signal recorded in enamel – namely less intense Sr/Ca fluctuations and lower values in *H. erectus* compared to *Pongo* sp. – also suggest that *H. erectus* was less tied to certain seasonal staple-foods than *Pongo.* Indeed, *H. erectus* appears to have been more flexible in its diet than *Pongo* sp., suggesting exploitation of diverse resources throughout the year that were available in the Indonesian

palaeolandscape. In turn, this could indicate that *H. erectus* had more complex social behaviours with the ability of provisioning and sharing food equally within the group, thus allowing to maintain daily calorie intake[72,83,84] and having low intra-tooth Sr/Ca variability. Furthermore, nearly 70 km East of Sangiran, at the site of Trinil where *H. erectus* was first discovered and described, it was suggested that members of this species likely consumed aquatic resources like shellfish, indicating a high level of food resilience[85]. Lower Sr/Ca episodes suggest the consumption of more meat-based diet, whereas elevated ratios could be linked to additional plant-based resources and/or underground storage organs, which can be found all year round[86] possessing higher Sr/Ca ratios[87,88].

Conclusions

Distinct differences in the chemical pattern of cyclical food resource availability point to life history and behavioral differences of Pleistocene Southeast Asian penecontemporaneous *Pongo* sp. and *H. erectus*, both reacting to seasonal changes in different ways. Orangutans are low-energy specialists who avoid nutritional scarce periods by decreasing their daily energy demands. This lifestyle might be indicated by temporary substantial increases of the Sr/Ca ratio that possibly imply seasonal food availability during monsoon seasons.

While *Pongo* sp. presumably consumed food resources locally available in lowland forests, *H. erectus* was more versatile, more mobile and exploited a broader range of high diversity food resources that were available at a regional scale. We conclude, that *H. erectus* was able to alleviate seasonal effects of nutritional changes by developing strategies aiming at exploiting a wide spectrum of high-quality food resources, possibly in relation with complex social structures enabling an equally distributing of gathered resources among the members of the group.

As *H. erectus* might not have been able to survive longer periods of low food availability, its dietary behaviors differ distinctly from earlier members of the genus *Homo.* In the absence of any other direct evidence of *H. erectus* behavior, our results indicate a high level of planning and resilience of *H. erectus* on Java. Our results underline the importance of fossilized hard tissue chemical analysis of early humans at daily time-resolution for understanding the behavioral past and the expansion of human capacities.

Methods

Overall the methodologies employed here follow those in Nava et al. 2020[14] and Müller et al. 2019[22] and only a brief summary is given here below.

Enamel thin sections. Preparation, imaging and histological analysis of enamel thin sections[89,90] were carried out at the Museo delle Cività in Rome. Sectioning was performed using a Leica high precision diamond blade (Leica AG) and IsoMet low speed diamond blade microtome (Buehler Ltd). Sections were ground with Minimet 1000 Automatic Polishing Machine (Buehler Ltd) using silicon carbide grinding

papers with two grits (1000 and 2500) (Buehler Ltd). Sections were polished using a Minimet 1000 Automatic Polishing Machine (Buehler Ltd) with a micro-tissue damped with distilled water and diamond paste (Diamond DP-suspension M, Struers) containing 1 µm sized monocrystalline diamonds. Thickness of the faunal thin sections was 130–150 µm depending on the preservation and visibility of the enamel microstructure. The hominid section thickness varied between 250 and 400 µm, thus facilitating potential future isotopic analysis.

LA-ICPMS analyses. LA-ICPMS analyses were carried out at the Frankfurt Isotope and Element Research Centre (FIERCE), Goethe University (Frankfurt am Main). Histologically-controlled tracks were determined on the enamel micrographs with Photoshop (Adobe Inc.). Sampling included continuous laser ablation tracks in enamel <100µm parallel to the EDJ starting from the tip of the dentine horn towards the cervical margin of the tooth crown[22].

The LA-ICPMS system includes an 193nm ArF excimer laser (RESOlution S-155; now Applied Spectra, Inc. (ASI), USA) coupled to a two-volume laser ablation cell (Laurin Technic, Australia)[22]. The laser ablation system is connected to an ICPMS Element XR^{TM} (Thermo Fisher Scientific) using nylon6-tubing. Thin sections were ultrasonically cleaned with methanol and fixed in the sample holder together with a series of primary and secondary standards. The micrographs with pre-marked laser tracks were uploaded in GeoStar µGIS Software (Norris Scientific, Australia) and retraced before LA-analyses. LA-ICPMS data acquisition was performed in continuous path mode due to the benefits of a two-volume LA cell with fast signal washout and constant signal response[22,91].

Prior to analysis, laser tracks were cleaned with a bigger spot size (40 µm), higher repetition rate (20 Hz) and scan speed (varying between 16.7-30 µm/s depending on the size of teeth) to remove surface residues, which could alter the results[92]. Analyses were carried out with a spot size of 18 µm, scan speed of 10 µm/s and a repetition rate of 15 Hz. The time signal obtained from the ICPMS can be directly transferred to distance along the LA tracks via the constant scan speed of the laser X-Y stage; no time delays of the X-Y stage exist at waypoints of composite tracks[22]. Between the LA system and the ICPMS, a signal smoothing device (“squid”) is incorporated[91].

The ICPMS (Element XR) detected the following isotopes from the ablated sample material (m/z):^{25}Mg, ^{27}Al, ^{43}Ca, ^{44}Ca, ^{66}Zn, ^{86}Sr, ^{88}Sr, ^{89}Y, ^{138}Ba, ^{140}Ce, ^{208}Pb, ^{238}U. For calibration purposes (following Longerich et al. 1996[93]), NIST612 as a primary external standard and ^{44}Ca as internal standard were used. In bioapatite, Ca is commonly used as an internal standard, which is set at 37%[22,94,95], but for elemental ratios no prior knowledge of sample [Ca] is necessary. For NIST 612 the following preferred values (± 2SD (in %)) were used (from GeoREM website http://georem.mpch-mainz.gwdg.de): CaO: 11.9 ± 0.4%m/m; Zn: 38 ± 4, Sr: 78.4 ± 0.2, Y: 38 ± 2, Ba: 39.7 ± 0.4, Ce: 38.7 ± 0.4, Pb: 38.57 ± 0.2, U: 37.38 ± 0.08 µg/g.

Secondary standards with known concentrations and a matrix broadly similar to apatite (STDPx glasses) were analysed to assess accuracy and precision: STDP3-150, STDP3-1500, STDP5 (Ca-P-(Si) glass standards)[96], KL2-G (basalt glass)[97], MAPS5 (phosphate pellet) and MACS3 (Microanalytical Carbonate Standard) (United States Geological Survey USGS: preliminary Certificate of Analysis by Steve Wilson), both available as 'nano'pellets from D. Garbe-Schönberg[98,99]. MACS3 was used for Zn accuracy because no reported Zn values are available for the Ca-P-(Si) glass standard[22]. Comparisons between measured secondary standard concentrations and reported concentrations revealed that the most accurate results with the lowest average bias were the combination of NIST612 with ^{44}Ca. Average relative biases of all three STDPx standards and MAPS5 were (in %): Al: -2.87 ± 3.26, Ca: 2.62 ± 1.72, Rb: 2.14 ± 20.47, Sr: 2.57 ± 4.98, Y: 5.85 ± 3.11, Ba: 0.68 ± 5.23, Ce: -1.31 ± 3.46, Pb: -2.88 ± 10.33, U: 2.80 ± 5.48 (average bias of all standards ± 1SD in %).

The compositional profiles displaying the concentration of elements relative to distance/days along the EDJ profile were smoothed with a locally weighted polynomial regression fit, with its associated standard error range (±2 SE) for each predicted value[100]. The software R (ver. 4.0.4; R-Core-Team, 2021) and the packages "lava", "readxl", "shape" and "tidyverse" were used for all statistical computations and generation of graphs.

Elemental data was matched with odontochronologies of the *H. erectus* and *Pongo* sp. specimens by chronologizing each EDJ track after LA-ICPMS analysis, and directly assessing the enamel daily secretion rates (DSR, i. e. the speed at which the ameloblast - the enamel forming cells - move towards the outer surface of the tooth, expressed in µm day^{-1}) along the prisms[101,102], in the 100 µm region close to the EDJ. Carefully chosen histologically-defined (EDJ) profiles facilitate the correlation between odontochronological and geochemical signals at very high time resolution (<1 week).

Declarations

Acknowledgements

We express our gratitude to the Werner Reimers Foundation in Bad Homburg, which provides the Gustav Heinrich Ralph von Koenigswald collection as a permanent loan for scientific research to the Senckenberg Research Institute and Natural History Museum Frankfurt. FIERCE, where all analyses were performed, is financially supported by the Wilhelm and Else Heraeus Foundation and by the Deutsche Forschungsgemeinschaft (DFG, INST 161/921-1 FUGG and INST 161/923-1 FUGG), which are gratefully acknowledged. We thank Linda Marko and Axel Gerdes for help with analytical work. We thank Rainer Brocke and Gunnar Riedel for assistance with microscopic imaging. C. Z. acknowledges the support of the French CNRS (Centre National de la Recherche Scientifique). J.K. received funding from the Erasmus+ Traineeship program (2019). A. N. and J. K. received funding from the European Union's Horizon 2020 research and innovation programme under the Marie Skłodowska-Curie grant agreement (A. N.: No.842812, J. K.: No.861389).

Author contributions

The study was initiated by J.K. during her MSc research project under the supervision of W. M., L. B. and A. N.; J. K., W. M., A. N., L. B., F. S. and O. K. designed research; J. K., W. M., A. N., L. B., B. P. and R. A. performed research, J. K., W. M., A. N. and L. B. analyzed data, J. K., W. M., F. S., O. K., C. Z., L. B. and A. N. wrote the manuscript with contribution from all other authors.

Data availability

The raw data of element analyses used in this study are available as a separate Excel file.

Competing interests

The authors declare no competing interests.

Additional Information

Supplementary information is available in the online version of the paper.

Reprints and permissions information is available at www.nature.com/reprints.

Correspondence and requests for materials should be addressed to J. K. (juelide.kubat@gmail.com), A. N. (alessianava@gmail.com) and W.M. (w.muller@em.uni-frankfurt.de).

References

1. von Koenigswald, G. H. R. Fossil hominids from the Lower Pleistocene of Java. in *Rep. 18th Internat Geological Congress* 59–61 (1948).

2. Grine, F. E. & Franzen, J. L. Fossil hominid teeth from the Sangiran Dome (Java, Indonesia). *Cour. Forsch. Inst. Senckenberg* **171**, 75–103 (1994).

3. Bettis, E. A. *et al.* Way out of Africa: Early Pleistocene paleoenvironments inhabited by *Homo erectus* in Sangiran, Java. *J. Hum. Evol.* **56**, 11–24 (2009).

4. Matsu'ura, S. *et al.* Age control of the first appearance datum for Javanese *Homo erectus* in the Sangiran area. *Science* **367**, 210–214 (2020).

5. Weidenreich, F. Giant early man from Java and South China. *Anthropol. Pap. Am. Mus. Nat. Hist.* **40**, 1–134 (1945).

6. von Koenigswald, G. H. R. *Pithecanthropus*, *Meganthropus* and the Australopithecinae. *Nature* **173**, 795–797 (1954).

7. Franzen, J. L. What is "*Pithecanthropus dubius* Koenigswald, 1950"? In *Ancestors: The Hard Evidence* (ed Delson, E.) 221–226 (Alan R. Liss, Inc., New York, 1985).

8. Tyler, D. E. Sangiran 5, ("*Pithecanthropus dubius*"), *Homo erectus*, "*Meganthropus*," or *Pongo*? *Hum. Evol.* **18**, 229–241 (2003).

9. Tyler, D. E. An examination of the taxonomic status of the fragmentary mandible Sangiran 5, (*Pithecanthropus dubius*), *Homo erectus*, '*Meganthropus*', or *Pongo*? *Quat. Int.* **117**, 125–130 (2004).

10. Zanolli, C. *et al.* Evidence for increased hominid diversity in the Early to Middle Pleistocene of Indonesia. *Nat. Ecol. Evol.* **3**, 755–764 (2019).

11. Balter, V., Braga, J., Télouk, P. & Thackeray, J. F. Evidence for dietary change but not landscape use in South African early hominins. *Nature* **489**, 558–560 (2012).

12. Joannes-Boyau, R. *et al.* Elemental signatures of *Australopithecus africanus* teeth reveal seasonal dietary stress. *Nature* **572**, 112–115 (2019).

13. Smith, T. M. *et al.* Wintertime stress, nursing, and lead exposure in Neanderthal children. *Sci. Adv.* **4**, 9483–9514 (2018).

14. Nava, A. *et al.* Early life of Neanderthals. *Proc. Natl. Acad. Sci. USA* **117**, 28719–28726 (2020).

15. Hoppe, K. A., Koch, P. L. & Furutani, T. T. Assessing the preservation of biogenic strontium in fossil bones and tooth enamel. *Int. J. Osteoarchaeol.* **13**, 20–28 (2003).

16. Hinz, E. A. & Kohn, M. J. The effect of tissue structure and soil chemistry on trace element uptake in fossils. *Geochim. Cosmochim. Acta* **74**, 3213–3231 (2010).

17. Bromage, T. G., Hogg, R. T., Lacruz, R. S. & Hou, C. Primate enamel evinces long period biological timing and regulation of life history. *J. Theor. Biol.* **305**, 131–144 (2012).

18. Lacruz, R. S., Dean, M. C., Ramirez-Rozzi, F. & Bromage, T. G. Megadontia, striae periodicity and patterns of enamel secretion in Plio-Pleistocene fossil hominins. *J. Anat.* **213**, 148–158 (2008).

19. Lacruz, R. S., Habelitz, S., Wright, J. T. & Paine, M. L. Dental enamel formation and implications for oral health and disease. *Physiol. Rev.* **97**, 939–993 (2017).

20. Dean, M. C. Tooth microstructure tracks the pace of human life-history evolution. *Proc. R. Soc. B* **273**, 2799–2808 (2006).

21. Müller, W. & Anczkiewicz, R. Accuracy of laser-ablation (LA)-MC-ICPMS Sr isotope analysis of (bio)apatite-a problem reassessed. *J. Anal. At. Spectrom.* **31**, 259–269 (2016).

22. Müller, W. *et al.* Enamel mineralization and compositional time-resolution in human teeth evaluated via histologically-defined LA-ICPMS profiles. *Geochim. Cosmochim. Acta* **255**, 105–126 (2019).

23. Li, Q. *et al.* Spatially-resolved Ca isotopic and trace element variations in human deciduous teeth record diet and physiological change. *Environ. Archaeol.* 1–10 (2020). doi:10.1080/14614103.2020.1758988

24. Elias, R. W., Hirao, Y. & Patterson, C. C. The circumvention of the natural biopurification of calcium along nutrient pathways by atmospheric inputs of industrial lead. *Geochim. Cosmochim. Acta* **46**, 2561–2580 (1982).

25. Burton, J. H., Price, T. D. & Middleton, W. D. Correlation of bone Ba/Ca and Sr/Ca due to biological purification of Calcium. *J. Archaeol. Sci.* **26**, 609–616 (1999).

26. Balter, V. *et al.* Ecological and physiological variability of Sr/Ca and Ba/Ca in mammals of West European mid-Würmian food webs. *Palaeogeogr. Palaeoclimatol. Palaeoecol.* **186**, 127–143 (2002).

27. Pate, F. D. Bone chemistry and paleodiet. *J. Archaeol. Method Theory* **1**, 161–209 (1994).

28. Kohn, M. J., Morris, J. & Olin, P. Trace element concentrations in teeth - a modern Idaho baseline with implications for archeometry, forensics, and palaeontology. *J. Archaeol. Sci.* **40**, 1689–1699 (2013).

29. Janssen, R. *et al.* Tooth enamel stable isotopes of Holocene and Pleistocene fossil fauna reveal glacial and interglacial paleoenvironments of hominins in Indonesia. *Quat. Sci. Rev.* **144**, 145–154 (2016).

30. Peek, S. & Clementz, M. T. Sr/Ca and Ba/Ca variations in environmental and biological sources: A survey of marine and terrestrial systems. *Geochim. Cosmochim. Acta* **95**, 36–52 (2012).

31. Reynard, B. & Balter, V. Trace elements and their isotopes in bones and teeth: Diet, environments, diagenesis, and dating of archeological and paleontological samples. *Palaeogeogr. Palaeoclimatol. Palaeoecol.* **416**, 4–16 (2014).

32. Blumenthal, S. A. *et al.* Stable isotope time-series in mammalian teeth: In situ δ18O from the innermost enamel layer. *Geochim. Cosmochim. Acta* **124**, 223–236 (2014).

33. Zazzo, A., Balasse, M. & Patterson, W. P. High-resolution $\delta^{13}C$ intratooth profiles in bovine enamel: Implications for mineralization pattern and isotopic attenuation. *Geochim. Cosmochim. Acta* **69**, 3631–

3642 (2005).

34. Deutsch, D. & Pe'er, E. Development of enamel in human fetal teeth. *J. Dent. Res.* **61**, 1543–1551 (1982).

35. Guatelli-Steinberg, D., Ferrell, R. J. & Spence, J. Linear enamel hypoplasia as an indicator of physiological stress in great apes: Reviewing the evidence in light of enamel growth variation. *Am. J. Phys. Anthropol.* **148**, 191–204 (2012).

36. Lacruz, R. S., Dean, M. C., Ramirez-Rozzi, F. & Bromage, T. G. Megadontia, striae periodicity and patterns of enamel secretion in Plio-Pleistocene fossil hominins. *J. Anat.* **213**, 148–158 (2008).

37. Reid, D. J. & Dean, M. C. Variation in modern human enamel formation times. *J. Hum. Evol.* **50**, 329–346 (2006).

38. Smith, T. M. Dental development in living and fossil orangutans. *J. Hum. Evol.* **94**, 92–105 (2016).

39. Schwartz, G. T., Reid, D. J. & Dean, C. Developmental aspects of sexual dimorphism in hominoid canines. *Int. J. Primatol.* **22**, 837–860 (2001).

40. Bonhommeau, S. *et al.* Eating up the world's food web and the human trophic level. *Proc. Natl. Acad. Sci. USA* **110**, 20617–20620 (2013).

41. Sponheimer, M. & Lee-Thorp, J. A. Enamel diagenesis at South African australopith sites: Implications for paleoecological reconstruction with trace elements. *Geochim. Cosmochim. Acta* **70**, 1644–1654 (2006).

42. Eltringham, S. K. The pygmy hippopotamus (*Hexaprotodon liberiensis*). in *Pigs, Peccaries and Hippos* (ed Oliver, W.) 55–60 (International Union for the Conservation of Nature and Natural Resources, Gland, 1993).

43. Jablonski, N. G. The hippo's tale: How the anatomy and physiology of Late Neogene Hexaprotodon shed light on Late Neogene environmental change. *Quat. Int.* **117**, 119–123 (2004).

44. Hendier, A. Diet determination of wild pygmy hippopotamus (*Choeropsis liberiensis*). (University of Neuchâtel, Switzerland, 2019).

45. Klein, I. Ernährung und ökologisches Profil von *Axis lydekkeri*. (Goethe University Frankfurt, 2020).

46. Wagner, A. Rekonstruktion von Körpermassen pleistozäner Rhinocerotidae in der Sammlung von Koenigswald. (Univ.-Bibliothek Frankfurt am Main, 2007).

47. Thompson, J. C., Carvalho, S., Marean, C. W. & Alemseged, Z. Origins of the human predatory pattern: The transition to large animal exploitation by early hominins. *Curr. Anthropol.* **60**, (2019).

48. Ben-Dor, M., Sirtoli, R. & Barkai, R. The evolution of the human trophic level during the Pleistocene. *Am. J. Phys. Anthropol.* (2021). doi:10.1002/ajpa.24247

49. Storm, P. A carnivorous niche for Java Man? A preliminary consideration of the abundance of fossils in Middle Pleistocene Java. *C. R. Palevol* **11**, 191–202 (2012).

50. Sillen, A. & Kavanagh, M. Strontium and paleodietary research: A review. *Yearb Phys Anthropol.* **25**, 67–90 (1982).

51. Sillen, A. & Smith, P. Weaning patterns are reflected in strontium-calcium ratios of juvenile skeletons. *J. Archaeol. Sci.* **11**, 237–245 (1984).

52. Humphrey, L. T., Dean, M. C., Jeffries, T. E. & Penn, M. Unlocking evidence of early diet from tooth enamel. *Proc. Natl. Acad. Sci. USA* **105**, 6834–6839 (2008).

53. Humphrey, L. T. Isotopic and trace element evidence of dietary transitions in early life. *Ann. Hum. Biol.* **41**, 348–357 (2014).

54. Humphrey, L. T. Weaning behaviour in human evolution. *Semin. Cell Dev. Biol.* **21**, 453–461 (2010).

55. van Noordwijk, M. A., Willems, E. P., Utami Atmoko, S. S., Kuzawa, C. W. & van Schaik, C. P. Multi-year lactation and its consequences in Bornean orangutans (*Pongo pygmaeus wurmbii*). *Behav. Ecol. Sociobiol.* **67**, 805–814 (2013).

56. Kanamori, T., Kuze, N., Bernard, H., Malim, T. P. & Kohshima, S. Fluctuations of population density in Bornean orangutans (*Pongo pygmaeus morio*) related to fruit availability in the Danum Valley, Sabah, Malaysia: a 10-year record including two mast fruitings and three other peak fruitings. *Primates* **58**, 225–235 (2017).

57. Smith, T. M., Austin, C., Hinde, K., Vogel, E. R. & Arora, M. Cyclical nursing patterns in wild orangutans. *Sci. Adv.* **3**, e1601517 (2017).

58. Dean, C., Le Cabec, A., Spiers, K., Zhang, Y. & Garrevoet, J. Incremental distribution of strontium and zinc in great ape and fossil hominin cementum using synchrotron X-ray fluorescence mapping. *J. R. Soc. Interface* **15**, (2018).

59. Dean, M. C., Le Cabec, A., Van Malderen, S. J. M. & Garrevoet, J. Synchrotron X-ray fluorescence imaging of strontium incorporated into the enamel and dentine of wild-shot orangutan canine teeth. *Arch. Oral Biol.* **119**, 104879 (2020).

60. Pontzer, H., Raichlen, D. A., Shumaker, R. W., Ocobock, C. & Wich, S. A. Metabolic adaptation for low energy throughput in orangutans. *Proc. Natl. Acad. Sci. USA* **107**, 14048–14052 (2010).

61. Mahaney, W. C., Hancock, R. G. V, Aufreiter, S., Milner, M. W. & Voros, J. Bornean orangutan geophagy: analysis of ingested and control soils. *Environ. Geochem. Health* **38**, 51-64 (2016).

62. van Noordwijk, M. A. & van Schaik, C. P. Development of ecological competence in Sumatran orangutans. *Am. J. Phys. Anthropol.* **127**, 79–94 (2005).

63. Marshall, A. J. *et al.* Orangutan population biology, life history, and conservation. In *Orangutans: Geographic variation in behavioral ecology and conservation* (eds Wich, S. A., Suci Utami Atmoko, S., Mitra Setia, T. & van Schaik, C. P.) 311–326 (Oxford University Press, Oxford, 2009).

64. Galdikas, B. M. F. & Wood, J. W. Birth spacing patterns in humans and apes. *Am. J. Phys. Anthropol.* **83**, 185–191 (1990).

65. Leuser National Park, G., Sugardjito, J., te Boekhorst, J. A. & van Hooff, J. A. R. A. M. Ecological constraints on the grouping of wild orang-utans (*Pongo pygmaeus*) in the Gunung Leuser National Park, Sumatra, Indonesia. *Int. J. Primatol.* **8**, 17–41 (1987).

66. Wich, S. A. *et al.* Life history of wild Sumatran orangutans (*Pongo abelii*). *J. Hum. Evol.* **47**, 385–398 (2004).

67. Dean, C. *et al.* Growth processes in teeth distinguish modern humans from *Homo erectus* and earlier hominins. *Nature* **414**, 628–631 (2001).

68. Dean, M. C. & Liversidge, H. M. Age estimation in fossil hominins: Comparing dental development in early *Homo* with modern humans. *Ann. Hum. Biol.* **42**, 415–429 (2015).

69. Sémah, A.-M., Sémah B, F., Djubiantono, T. & Brasseur, B. Landscapes and hominids' environments: Changes between the Lower and the early Middle Pleistocene in Java (Indonesia). *Quat. Int.* **4**, 451 (2009).

70. Sémah, A. M. & Sémah, F. The rain forest in Java through the Quaternary and its relationships with humans (adaptation, exploitation and impact on the forest). *Quat. Int.* **249**, 120–128 (2012).

71. Brasseur, B., Sémah, F., Sémah, A.-M. & Djubiantono, T. Approche paléopédologique de l'environnement des hominidés fossiles du dôme de Sangiran (Java central, Indonésie). *Quaternaire* **22**, 13–34 (2011).

72. Pontzer, H. Ecological energetics in early *Homo*. *Curr. Anthropol.* **53**, S346-S358 (2012).

73. Aiello, L. C. & Wheeler, P. The expensive-tissue hypothesis: The brain and the digestive system in human and primate evolution. *Curr. Anthropol.* **36**, 199–221 (1995).

74. Bramble, D. M. & Lieberman, D. E. Endurance running and the evolution of *Homo*. *Nature* **432**, 345–352 (2004).

75. Shipman, P. & Walker, A. The costs of becoming a predator. *J. Hum. Evol.* **18**, 373–392 (1989).

76. Foley, R. A. The evolutionary consequences of increased carnivory in hominids. In *Meat-eating and human evolution* (eds Stanford, C. B. & Bunn, H.T.) 305–331 (Oxford University Press, Oxford, 2001).

77. Plummer, T. W. & Bishop, L. C. Oldowan hominin behavior and ecology at Kanjera south, Kenya. *J. Anthropol. Sci.* **94**, 29–40 (2016).

78. Binford, L. R. Willow smoke and dogs' tails: Hunter-gatherer settlement systems and archaeological site formation. *Am. Antiq.* **45**, 4–20 (1980).

79. Kelly, R. L. Hunter-gatherer mobility strategies. *J. Anthropol. Res.* **39**, 277–306 (1983).

80. Ungar, P. S., Grine, F. E. & Teaford, M. F. Diet in early *Homo*: A review of the evidence and a new model of adaptive versatility. *Annu. Rev. Anthropol.* **35**, 209–228 (2006).

81. Tausch, J. A New Method for Examining Hominin Dietary Strategy: Occlusal Microwear Vector Analysis of the Sangiran 7 *Homo erectus* Molars. (Goethe University Frankfurt, 2011).

82. Tausch, J., Kullmer, O. & Bromage, T. G. A new method for determining the 3D spatial orientation of molar microwear. *Scanning* **37**, 446–457 (2015).

83. O'Connell, J. F., Hawkes, K. & Jones, N. G. B. Grandmothering and the evolution of *Homo erectus*. *J. Hum. Evol.* **36**, 461–485 (1999).

84. Wrangham, R. W., Jones, J. H., Laden, G., Pilbeam, D. & Conklin-Brittain, N. The Raw and the Stolen. *Curr. Anthropol.* **40**, 567–594 (1999).

85. Joordens, J. C. A. *et al. Homo erectus* at Trinil on Java used shells for tool production and engraving. *Nature* **518**, 228–231 (2015).

86. Larbey, C., Mentzer, S. M., Ligouis, B., Wurz, S. & Jones, M. K. Cooked starchy food in hearths ca. 120 kya and 65 kya (MIS 5e and MIS 4) from Klasies River Cave, South Africa. *J. Hum. Evol.* **131**, 210–227 (2019).

87. Sillen, A. & Lee-Thorp, J. A. Trace element and isotopic aspects of predator-prey relationships in terrestrial foodwebs. *Palaeogeogr. Palaeoclimatol. Palaeoecol.* **107**, 243–255 (1994).

88. Sponheimer, M., de Ruiter, D., Lee-Thorp, J. & Späth, A. Sr/Ca and early hominin diets revisited: New data from modern and fossil tooth enamel. *J. Hum. Evol.* **48**, 147–156 (2005).

89. Caropreso, S. *et al.* Thin sections for hard tissue histology: A new procedure. *J. Microsc.* **199**, 244–247 (2000).

90. Nava, A. Hominin dental enamel: an integrated approach to the study of formation, maturation and morphology. (Sapienza Università di Roma, 2017).

91. Müller, W., Shelley, M., Miller, P. & Broude, S. Initial performance metrics of a new custom-designed ArF excimer LA-ICPMS system coupled to a two-volume laser-ablation cell. *J. Anal. At. Spectrom.* **24**, 209–214 (2009).

92. Evans, D. & Müller, W. LA-ICPMS elemental imaging of complex discontinuous carbonates: An example using large benthic foraminifera. *J. Anal. At. Spectrom.* **28**, 1039–1044 (2013).

93. Longerich, H. P., Jackson, S. E. & Günther, D. Laser ablation inductively coupled plasma mass spectrometric transient signal data acquisition and analyte concentration calculation. *J. Anal. At. Spectrom.* **11**, 899–904 (1996).

94. Retief, D. H., Cleaton-Jones, P. E., Turkstra, J. & De Wet, W. J. The quantitative analysis of sixteen elements in normal human enamel and dentine by neutron activation analysis and high-resolution gamma-spectrometry. *Arch. Oral Biol.* **16**, 1257–1267 (1971).

95. Lacruz, R. S. Enamel: Molecular identity of its transepithelial ion transport system. *Cell Calcium* **65**, 1–7 (2017).

96. Klemme, S. *et al.* Synthesis and preliminary characterisation of new silicate, phosphate and titanite reference glasses. *Geostand. Geoanalytical Res.* **32**, 39–54 (2008).

97. Jochum, K. P. *et al.* Accurate trace element analysis of speleothems and biogenic calcium carbonates by LA-ICP-MS. *Chem. Geol.* **318–319**, 31–44 (2012).

98. Garbe-Schönberg, D. & Müller, S. Nano-particulate pressed powder tablets for LA-ICP-MS. *J. Anal. At. Spectrom.* **29**, 990–1000 (2014).

99. Jochum, K. P. *et al.* Nano-powdered calcium carbonate reference materials: significant progress for microanalysis? *Geostand. Geoanalytical Res.* **43**, 595–609 (2019).

100. Cleveland, W. S., Grosse, E. & Shyu, W. M. Local regression models. In *Statistical Models in S* (eds Chambers, J. M. & Hastie, T.) 309–376 (Chapman and Hall/CRC, New York, 1992).

101. Guatelli-Steinberg, D., Floyd, B. A., Dean, M. C. & Reid, D. J. Enamel extension rate patterns in modern human teeth: Two approaches designed to establish an integrated comparative context for fossil primates. *J. Hum. Evol.* **63**, 475–486 (2012).

102. Birch, W. & Dean, M. C. A method of calculating human deciduous crown formation times and of estimating the chronological ages of stressful events occurring during deciduous enamel formation. *J. Forensic Leg. Med.* **22**, 127–144 (2014).

Tables

Table 1 ▯ List of specimens from the GHR v. Koenigswald Collection used in the present study. The specimens are housed in the Department of Palaeoanthropology, Senckenberg Research Institute and Natural History Museum Frankfurt, Frankfurt a. M., Germany.

	Catalogue number	Taxonomic Identification	Dental Elements
PRIMATES	SMF/PA/S7-13	*Hominidae/Homo erectus*	left M^3
	SMF/PA/S7-37	*Hominidae/Homo erectus*	right P^4
	SMF/PA/F8865	*Hominidae/Homo erectus*	left M_2
	SMF/PA/F8864	*Hominidae/Pongo* sp.	right M_2
CARNIVORA	SMF/PA/F6664	Felidae/ *Panthera tigris oxignatha*	right P_4
	SMF/PA/F6666	Felidae/ *Panthera tigris oxignatha*	right M_1
PERISSODACTYLA	SMF/PA/F5941	Rhinoceratidae	left M_1
	SMF/PA/F5950	Rhinoceratidae	left M_2
ARTIODACTYLA	SMF/PA/F738	Suidae/ *Sus* sp.	right M^3
	SMF/PA/F869	Suidae/ *Sus* sp.	right M^3
	SMF/PA/F5077	Cervidae/ *Axis lydekkeri*	left M_2
	SMF/PA/F5258	Cervidae/ *Axis lydekkeri*	right P^3, M^1, M^2, M^3
	SMF/PA/F6	Hippopotamidae/ *Hexaprotodon* sp.	right M^2
	SMF/PA/F53	Hippopotamidae/ *Hexaprotodon* sp.	left M_2

Table 2 ▯ Cusp Formation Time and Retzius Periodicity of the hominid sample.

Catalogue number	Taxon	Tooth type	Cusp/aspect	Track lenght [µm]	Track Formation Time [years]	Retzius Periodicity [days]
SMF/PA/S7-13	*Homo erectus*	left M^3	paracone/buccal	4303	1.9	7 or 8*
SMF/PA/S7-13	*Homo erectus*	left M^3	protocone/palatal	3629	1.8	
SMF/PA/S7-37	*Homo erectus*	right P^4	protocone/palatal	6470	2.9	8 or 9***
SMF/PA/F8865	*Homo erectus*	left M_2	protoconid/buccal	6252	3.1	8 or 9*
SMF/PA/F8865	*Homo erectus*	left M_2	metaconid/lingual	3906	-****	
SMF/PA/F8864	*Pongo* sp.	right M_2	protoconid/buccal	6009	2.9	8***
SMF/PA/F8864	*Pongo* sp.	right M_2	metaconid/lingual	5660	3.7	

*based on local DSRs between adjacent Retzius lines and not direct counts of cross striations due to section thickness; ** reported in Lacruz et al 2008 for S7-37 M1; ***direct counts of cross striations; ****section plane off centre, cervical portion damaged.

Figures

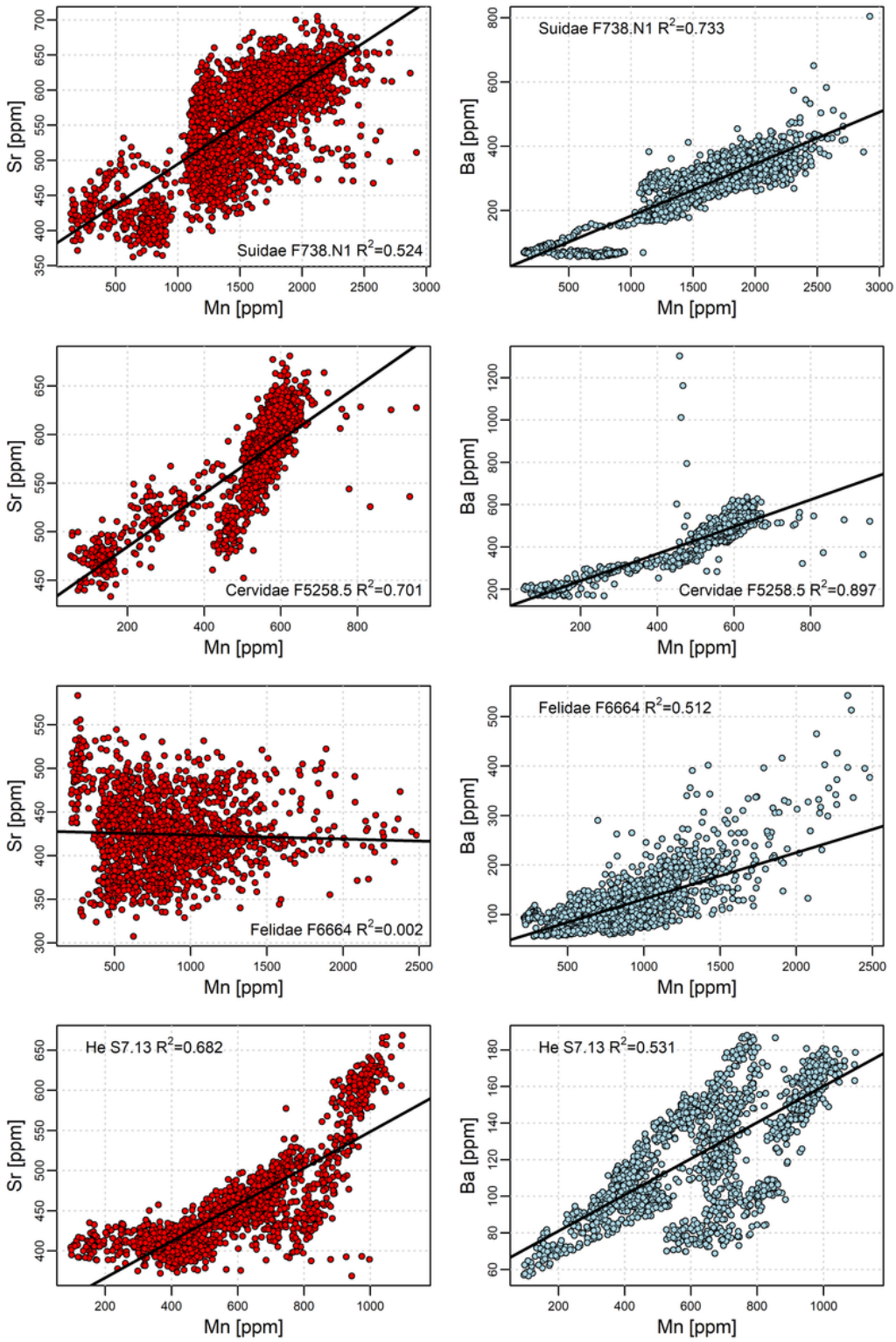

Figure 1

Scatter plots of Sr/Ca or Ba/Ca vs. [Mn] respectively for selected specimens, as representative of the diagenesis imprint in the fossil assemblage. See Supplementary Figure 3 for equivalent plots relative to [U].

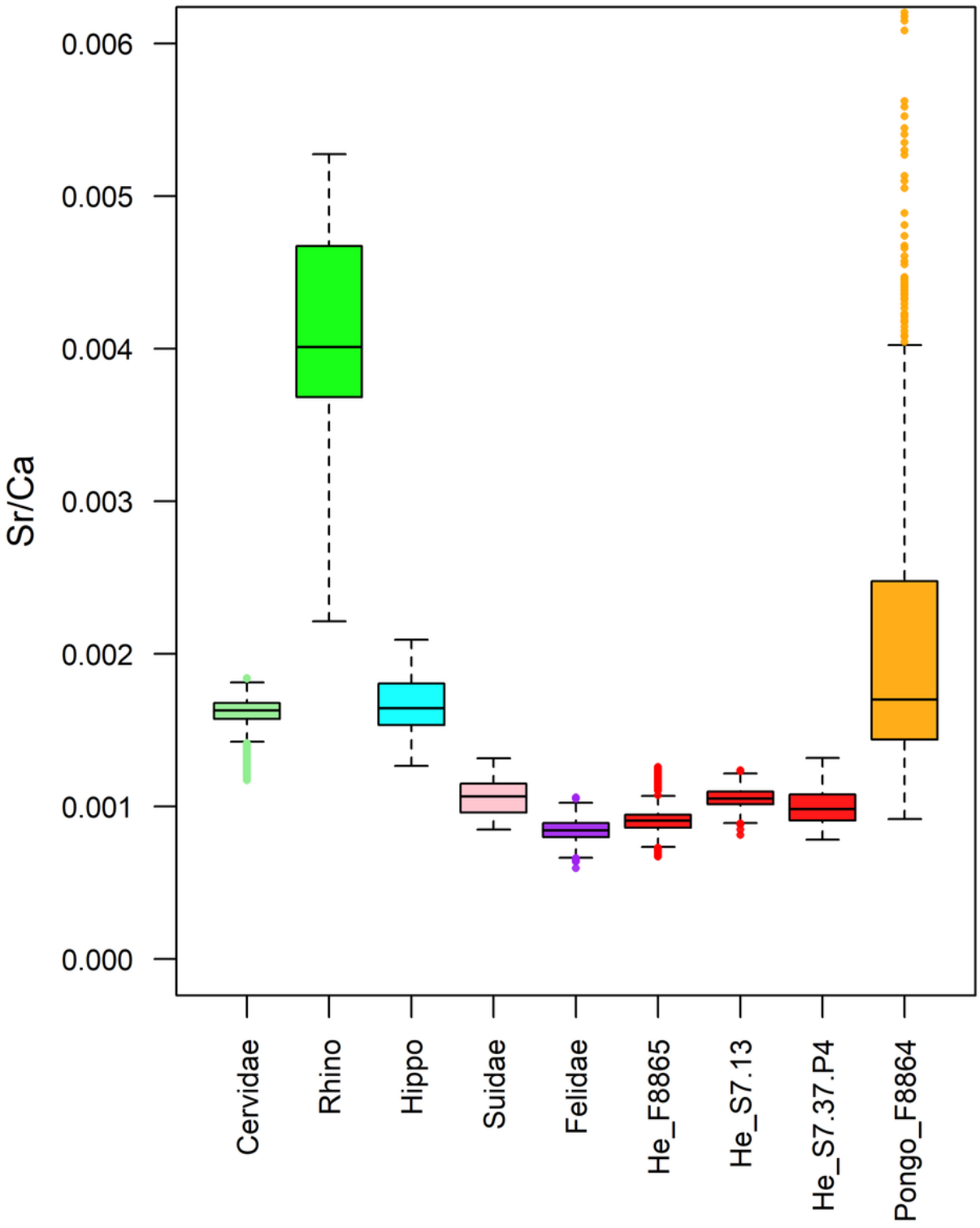

Figure 2

Sr/Ca ratios. Box plot comparing H. erectus and Pongo sp. specimens to those measured in other taxa with known trophic levels, all displayed after diagenesis filtering, i.e. [U]<1 ppm and [Mn]<400 ppm (µg/g).

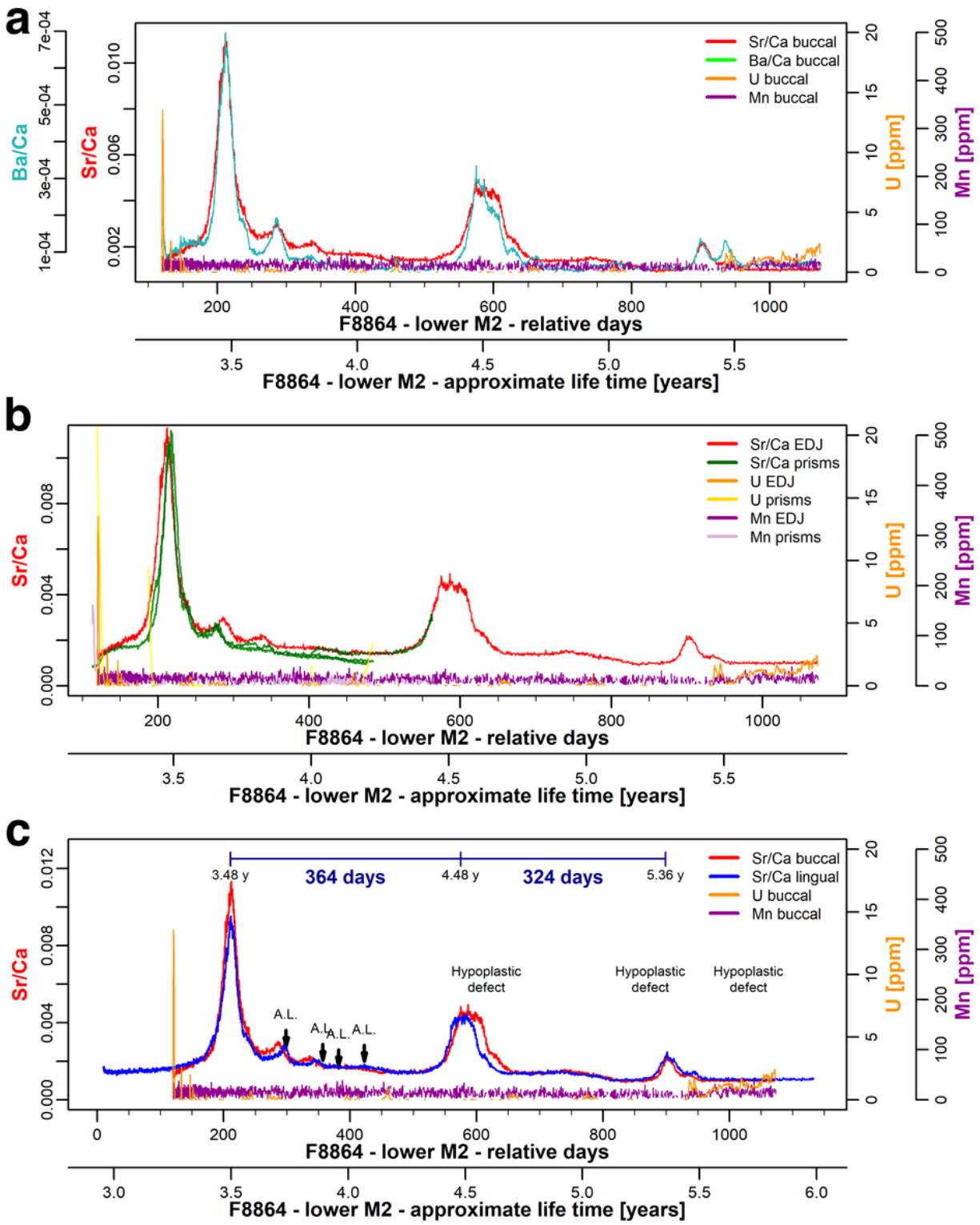

Figure 3

Sr/Ca, Ba/Ca, [U] and [Mn] signals in Pongo sp. F8864 molar. a, elemental signals at the EDJ level plotted against relative days; b, elemental signals along the EDJ and multiple prism profiles plotted against relative days; c, elemental signals on the mesiolingual and mesiobuccal cusp plotted against relative days. Accentuated lines (A. L.) and hypoplastic defects are highlighted.

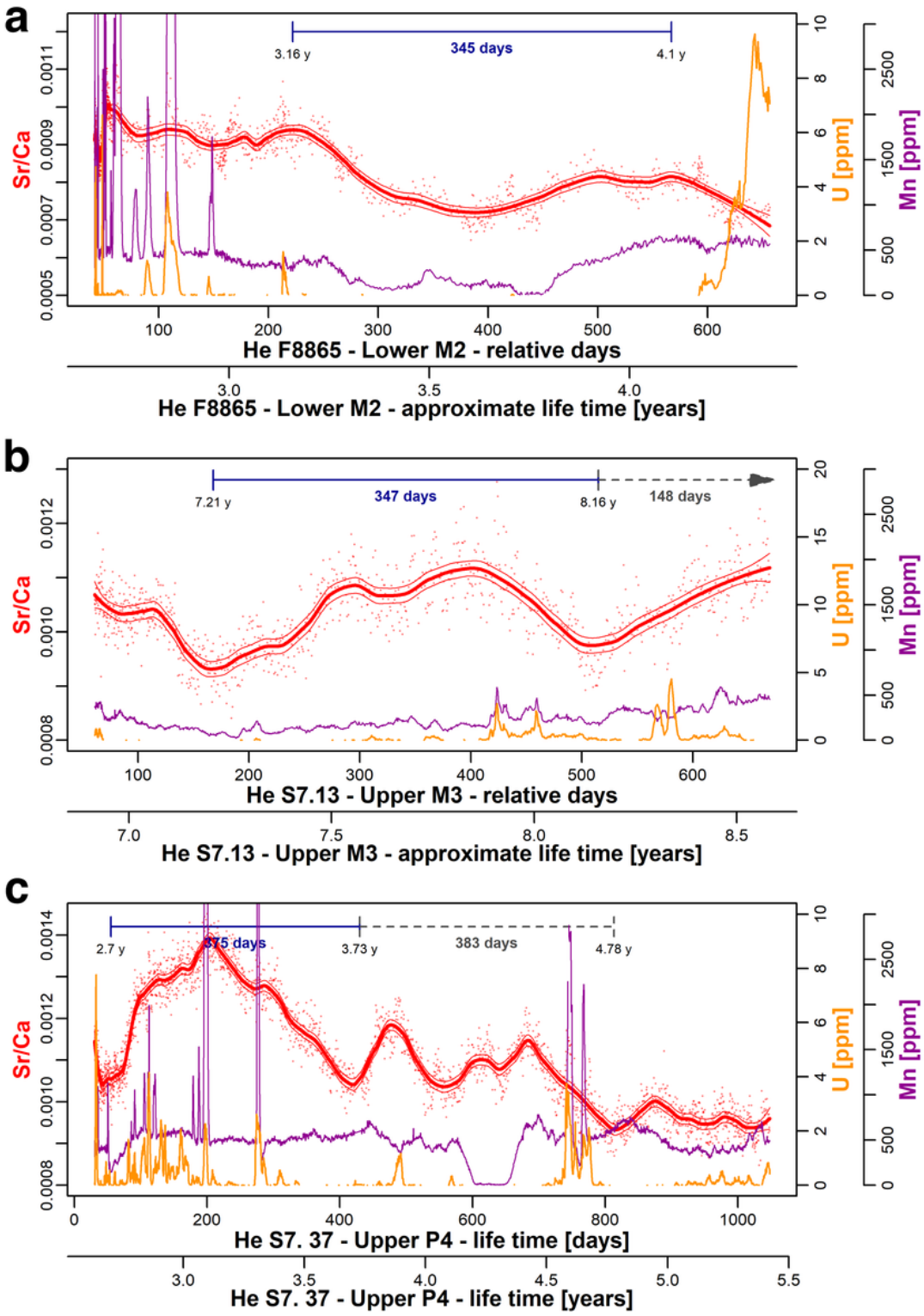

Figure 4

Compilation of Sr/Ca, [U] and [Mn] signals matched with the individual dental chronologies of H. erectus. a, F8865; b, S7-13; c, S7-37

Supplementary Files

This is a list of supplementary files associated with this preprint. Click to download.

- SOMKubat.docx
- SOMKubat.xlsb